The curcumin analog HO-3867 selectively kills cancer cells by converting mutant p53 protein to transcriptionally active wildtype p53

Esha Madan[a,b], Taylor M. Parker[c1], Matthias R. Bauer[d1], Alisha Dhiman[e], Christopher J. Pelham[f], Masaki Nagane[g], M. Lakshmi Kuppusamy[h], Matti Holmes[i], Thomas R. Holmes[i], Kranti Shaik[i], Kevin Shee[h], Salome Kiparoidze[j], Sean D. Smith[i], Yu-Soon A. Park[i], Jennifer J. Gomm[k], Louise J. Jones[k], Ana R. Tomás[a], Ana C. Cunha[a], Karuppaiyah Selvendiran[l], Laura A. Hansen[i], Alan R. Fersht[d], Kálmán Hideg[†m], Rajan Gogna[a,b2], and Periannan Kuppusamy[h3]

From the [a]Champalimaud Research, Champalimaud Centre for the Unknown, 1400-038 Lisbon, Portugal, the [b]Amity Institute of Molecular Medicine and Stem Cell Research, Amity University, Gautam Buddha Nagar Section 125, Noida 201301, India, the [c]Department of Surgery, Simon Cancer Research Center, Indiana University School of Medicine, Indianapolis, Indiana 46202, the [d]Medical Research Council Laboratory of Molecular Biology, Cambridge CB2 0QH, United Kingdom, the [e]Department of Medicinal Chemistry and Molecular Pharmacology, Purdue University, West Lafayette, Indiana 47907, the [f]Department of Pharmacology and Physiology, Saint Louis University, St. Louis, Missouri 63104, the [g]Department of Biochemistry, School of Veterinary Medicine, Azabu University, 1-17-71 Fuchinobe, Chuo-ku, Sagamihara, Kanagawa 252-5201, Japan, the [h]Department of Radiology and Medicine, Norris Cotton Cancer Center, Geisel School of Medicine, Dartmouth College, Lebanon, New Hampshire 03756, the [i]Department of Biomedical Sciences, Creighton University, Omaha, Nebraska 68178, the [j]Tbilisi State Medical University, Tbilisi 0179, Georgia, the [k]Centre for Tumour Biology, Barts Cancer Institute, Charterhouse Square, London, EC1M 6BQ, United Kingdom, the [l]Department of Obstetrics and Gynecology, College of Medicine, The Ohio State University, Columbus, Ohio 43210, and the [m]Institute of Organic and Medicinal Chemistry, Faculty of Sciences, University of Pécs, Pécs-H-7624, Hungary

Edited by Eric R. Fearon

p53 is an important tumor-suppressor protein that is mutated in more than 50% of cancers. Strategies for restoring normal p53 function are complicated by the oncogenic properties of mutant p53 and have not met with clinical success. To counteract mutant p53 activity, a variety of drugs with the potential to reconvert mutant p53 to an active wildtype form have been developed. However, these drugs are associated with various negative effects such as cellular toxicity, nonspecific binding to other proteins, and inability to induce a wildtype p53 response in cancer tissue. Here, we report on the effects of a curcumin analog, HO-3867, on p53 activity in cancer cells from different origins. We found that HO-3867 covalently binds to mutant p53, initiates a wildtype p53-like anticancer genetic response, is exclusively cytotoxic toward cancer cells, and exhibits high anticancer efficacy in tumor models. In conclusion, HO-3867 is a p53 mutant–reactivating drug with high clinical anticancer potential.

p53 is one of the most frequently mutated genes in cancer, and its loss of activity has been associated with oncogenic progression in multiple cancers (1, 2). The p53 transcription factor regulates oncogenic progression via multiple mechanisms that involve, but are not restricted to, cell cycle arrest, senescence, and apoptosis (3–5). Recent discoveries indicate that the transcriptional activity of p53 also determines important biological processes such as metabolism via regulation of *tigar* (6–8) and *sco2* (8–10), embryonic development of cardiomyocytes through Nkx2.5 and troponin T2 (11), and non-cell autonomous signaling in the tumor microenvironment (12), suggesting a critical role for p53 in the regulation of basic processes of human biology. Truncation (13) and transactivation domain (14), DNA-binding domain (15), and tetramerization domain mutations in the *p53* gene (16) impair the ability of p53 to interact with chromatin (17, 18). This eventually results in the loss of p53 transcriptional activity toward downstream effector genes involved in anticancer signaling (2, 13, 19). Loss of p53 activity via mutations is associated with metastasis and poor prognosis in breast cancer (20, 21), pancreatic cancer (2, 22), astrocytoma and oligoastrocytoma (23), and stage 1 non-small-cell lung carcinoma (24). Because mutant p53 ($p53^{MT}$) can accelerate neoplastic progression, addressing the *in situ* mutational status of *p53* may be indispensable for successful anticancer therapy (2, 3, 25, 26). In conclusion, $p53^{MT}$ promotes aggressive tumor phenotypes (2, 3), which suggests that the targeting of $p53^{MT}$ is an important anticancer strategy. Several clinical trials have been based on strategies to reintroduce wildtype p53 copies into cancerous tissues (27–29). In addition, there have been several clinical attempts to use molecular chaper-

ones that can rescue wildtype p53 (30–33). Because of the oncogenic role of mutant p53 (3, 26), reactivation of transcriptionally inactive mutant p53 is a promising approach to cancer therapy (30).

In the past few years, approaches involving drug-assisted reactivation of p53^{MT} have been adopted to achieve a gain of *p53* function for anticancer effects (34–39). However, an efficient anticancer drug that is both specific for binding p53^{MT} and nontoxic to normal cells has not been identified. Recently, mutant p53-reactivating drugs such as PRIMA-1 have been shown to bind to p53 via SH$_2$ linkage and refold the mutated forms to transcriptionally active DNA-binding forms to exert anticancer action (40, 41). A clinical trial with PRIMA-1 under the name APR-246 has shown an ability to induce changes in gene expression but with little clinical significance, possibly owing to the small number of study participants (38). Another example, RITA, a candidate p53-interacting and -activating drug (43), was later shown by NMR not to bind to p53 (44). Chetomin reactivates p53^{R175H} by increasing p53 and Hsp40 interaction (45), although chetomin also has nonspecific p53 effects (46). CP-31398 (47), another putative p53^{MT}-activating molecule, does not actually bind p53^{MT} but instead interacts with DNA, destabilizes the DNA–p53 core– domain complex, and causes nonspecific toxicity in cancer cells (48, 49). Other small molecules, such as NSC319726, STIMA-1, and SCH529074 (3), with the potential to restore the wildtype activity of mutant p53 are in the early stages of development and testing.

Here we show the potential of a novel curcumin analog HO-3867 (50) to bind with and reactivate p53^{MT} in cancer cells and tumor xenografts. HO-3867, a novel diarylidenyl piperidone compound and a curcumin analog, has been developed by incorporating a piperidone link to the β-diketone structure and fluoro-substitutions on the phenyl groups (50). The chemical design of HO-3867 includes a hydroxylamine group (=NOH) (Fig. S1*a*), which is converted to a biologically active nitroxide (=NO) form, specifically in the redox-rich environment of cancer cells (Fig. S1*b*) (50). Previously, we have shown that HO-3867 targets other p53-regulated and signaling-related genes (51). HO-3867 activates p53 (52) and thus effectively and specifically inhibits the constitutive activation of STAT3 (50), most likely by mechanisms described previously (53). Another possible p53 downstream effect of HO-3867 has been observed via the activation of PTEN expression followed by the inhibition of Akt activation, cell-cycle arrest, and apoptosis (52). HO-3867 also has been shown to inhibit ovarian cancer cell migration and invasion by altering FAS/FAK expression and by inhibiting vascular endothelial growth factor signaling in a p53-dependent manner (50). In the present study, we demonstrated a novel role for HO-3867 as a p53-activating compound that is exclusively cytotoxic toward cancer-derived cells. HO-3867 directly bound to p53^{MT} *in vitro*, activated the p53 transcriptional pathway in cancer cells of multiple origins with a broad spectrum of p53 DNA-binding domain mutations, and exhibited anticancer activity in *p53^{MT}* cancer models.

Results and discussion

Because of concerns regarding toxicity toward healthy (noncancerous) cells (38, 39), we developed a clinically derived model to assess the nonspecific cytotoxicity of HO-3867 toward various human cell types. The cytotoxicity of HO-3867 (10 μM) was examined in heterogeneous primary cultures derived from (i) human breast, colon, and liver normal and cancer tissues (Fig. 1*a*); (ii) stromal fibroblasts derived from breast tissue adjacent to cancer (Fig. 1*a*); and (iii) chemo- and radiosensitive tissues such as lymphoid and GI tract (Fig. 1*a*). Flow cytometric analysis showed small apoptotic population upon HO-3867 treatment of cell derived from normal tissues or normal breast fibroblasts or to radiosensitive lymphoid and GI tract tissues (Fig. 1*b*). However, HO-3867 exclusively induced apoptosis in cancer cells of breast, colon, and liver origin (Fig. 1*b*). Cisplatin was cytotoxic to both normal and cancer cells of all origins (Fig. 1*b*). A *p53* mutational analysis in the breast, colon, and liver cancer samples showed the presence of distinct DNA-binding domain (DBD)[4] mutations in each case (Fig. 1*c*). The different cancer types harbored unique mutations spanning the p53 DBD, and primary cultures were sensitive to HO-3867–induced cytotoxicity. These data suggest that HO-3867 acts to halt cancer cell proliferation induced by p53 DBD mutant variants. Also, these data suggest that HO-3867 is a safe drug with limited cytotoxicity to normal cells while exhibiting a high anticancer apoptotic activity. Next, we further analyzed the *p53^{MT}*-specific cytotoxicity of HO-3867 (10 μM). Cellular apoptosis was measured in four *p53^{MT}* (A431, MDA-MB-468, WRO, and DU-145) and two *p53$^{-/-}$* (MCF-7 p53$^{-/-}$ and HCT p53$^{-/-}$) cancer lines. HO-3867 induced significant apoptosis in *p53^{MT}* cells, which was reversed by shRNA-mediated *p53* knockdown (Fig. 1*d*, inset). HO-3867 was ineffective at inducing apoptosis in *p53$^{-/-}$* cells. However, HO-3867 induced significant apoptosis in *p53$^{-/-}$* cells upon exogenous addition of *p53^{MT}* (Fig. 1*d*). These data suggest that HO-3867 induces cytotoxicity and anticancer activity in a *p53^{MT}*-dependent manner.

Because HO-3867 induced apoptosis in *p53^{MT}* cells, we evaluated whether there was any direct binding between HO-3867 and p53^{MT} under *in vitro* conditions. ^{1}H-^{15}N heteronuclear single-quantum coherence (HSQC) NMR experiments revealed that HO-3867 induces several chemical shift perturbations, especially in close proximity to the solvent-exposed cysteine 277 of the DBD (residues 94–312) of p53^{MT} Y220C (Fig. 2, *a* and *b*), suggesting a covalent binding mode. A comparison of the HSQC spectra after 20 or 150 min of incubation with HO-3867 at room temperature also revealed time-dependent chemical shift perturbations in the spectra, which is in line with the putative covalent binding to p53^{MT} Y220C (Fig. 2*c*). Electrospray ionization (ESI) mass spectrometry experiments showed a mass increase of 713 and 1426 Da after incubating the p53^{MT}-Y220C DBD with HO-3867 for 4 h at room tempera-

---

[4] The abbreviations used are: DBD, DNA-binding domain; HSQC, heteronuclear single-quantum coherence; ESI, electrospray ionization; qPCR, quantitative real-time PCR; RE, response element; GI, gastrointestinal; FBS, fetal bovine serum; NMR, nuclear magnetic resonance; MT, mutant; HRP, horseradish peroxidase; ANOVA, analysis of variance.

a

i) Cancer and Normal Tissue

ii) Stromal Tissue   **iii) Radiosensitive Tissue**

Breast   **Colon**   **Liver**   **Lymphoid tissue**   **GI tract tissue**

Tumor excised   Tumor excised   Tumor excised

b

Breast Normal | Breast Cancer | Colon Normal | Colon Cancer | Liver Normal | Liver Cancer | Breast Stromal Fibroblasts | Lymphoid Healthy | GI Tract Healthy

Percent Apoptosis (y-axis 0–100)

Conditions: Control, HO-3867, Cisplatin

P-values shown: P<0.01; P<0.001; P<0.01; P<0.01 and P<0.01; P<0.01; P<0.01 and P<0.05; P<0.001 and P<0.01; P<0.001 and P<0.01; P<0.01 and P<0.05

c

Breast Cancer

N-terminal domain (1-97)

5′ PSQKTYQGSYGFRLGFLHSGTAKSVTCTYSPALNKMFCQLAKTCPVQLWVDSTPPPGTRVRAMAIYKQSQHMTEVVRRCPHHERCSDSDGLAPPQHLIRVEGNLRVEYLDDRNTFRHSVVVPYEPPEVGSDCTTIHYNYMCNSSCMGGMNRRPILTIITLEDSSGNLLGRNSFEVRVCACPGRDRRTEEENLRKK 3′

^{271}G D G E N L^{289} (G A H G L mutations)

DNA binding domain (98-292)

C-terminal domain (293-393)

Colon Cancer

N-terminal domain (1-97)

5′ PSQKTYQGSYGFRLGFLHSGTAKSVTCTYSPALNKMFCQLAKTCPVQLWVDSTPPPGTRVRAMAIYKQSQHMTEVVRRCPHHERCSDSDGLAPPQHLIRVEGNLRVEYLDDRNTFRHSVVVPYEPPEVGSDCTTIHYNYMCNSSCMGGMNRRPILTIITLEDSSGNLLGRNSFEVRVCACPGRDRRTEEENLRKK 3′

^{163}N

DNA binding domain (98-292)

C-terminal domain (293-393)

Liver Cancer

N-terminal domain (1-97)

5′ PSQKTYQGSYGFRLGFLHSGTAKSVTCTYSPALNKMFCQLAKTCPVQLWVDSTPPPGTRVRAMAIYKQSQHMTEVVRRCPHHERCSDSDGLAPPQHLIRVEGNLRVEYLDDRNTFRHSVVVPYEPPEVGSDCTTIHYNYMCNSSCMGGMNRRPILTIITLEDSSGNLLGRNSFEVRVCACPGRDRRTEEENLRKK 3′

^{107}D

DNA binding domain (98-292)

C-terminal domain (293-393)

d

+ HO-3867

P<0.001

Percent Apoptosis (y-axis 0–100)

P<0.001

Inset Western blots: MCF-7 p53$^{-/-}$ (Con, +p53^{MT}): P53 (66, 45), GAPDH (45, 35); MCF-7 (Con, p53 shRNA): P53, GAPDH

+ p53^{MT} cDNA

Control | +p53 shRNA | + p53^{MT} cDNA | (+HO-3867 groups) | +p53 shRNA | + p53^{MT} cDNA

Cell lines: A-431, MDA-MB-468, WRO, DU-145, MCF-7 p53(-/-), HCT p53 (-/-)

p53^{MT} cells | p53-null cells

ture, confirming covalent modification of p53^{MT} (Fig. 2c). Additionally, the observed mass increase of 713 Da suggests that HO-3867 covalently modifies p53 as a dimer. Further experiments with cysteine to serine mutants (C277S/C182S, C124S/C182S, and C124S/C277S) of the p53 DBD revealed that the compound specifically reacts with cysteine 182 and cysteine 277 (Fig. 2d). Thus, covalent binding of HO-3867 to p53^{MT}-Y220C was observed based on structural affinities. We also expect HO-3867 will bind to and modify other DBD mutant variants.

After confirming the covalent binding of HO-3867 with p53^{MT} protein, the *p53^{MT}*-specific anticancer effects of HO-3867 (20 mg/kg body weight) were determined in *p53^{WT}* (MCF-7), *p53^{MT}* (A-431), and *p53$^{-/-}$* (MCF-7 p53$^{p53-/-}$) cell line–induced tumor xenografts (Fig. 3). The *top row* of Fig. 3a (control) shows the tumor growth of *p53 p53^{WT}*, *p53^{MT}*, and *p53$^{-/-}$* untreated xenografts after 28 days; the *second row* shows a significant reduction in tumor size when *p53^{WT}*, *p53^{MT}*, and *p53$^{-/-}$* xenografts were treated with HO-3867 along with exogenous addition of lentiviral particles coding for *p53^{WT}* cDNA. No significant effect on tumor growth (size) was observed upon vehicle treatment (*third row*) or upon treatment with lentiviral particles encoding expression of p53 shRNA (*fourth row*) (Fig. 3a). *p53^{WT}* and *p53^{MT}* tumors treated with HO-3867 were significantly smaller than the corresponding untreated tumors (*fifth row versus first row*, Fig. 3a). The *p53$^{-/-}$* tumors did not show similar responsiveness to HO-3867 treatment (Fig. 3a, *fifth row*, *far right*) and were larger than the tumors with *p53^{WT}* and *p53^{MT}* status (*fifth row*, *left* and *center*). When the *p53^{WT}* and *p53^{MT}* tumors were treated with HO-3867 along with lentiviral particles coding for p53 shRNA, larger tumors were observed upon *p53* silencing (Fig. 3a, *sixth row*). *p53$^{-/-}$* cells were treated with HO-3867 along with lentiviral particles encoding for *p53^{MT}* cDNA (Fig. 3a, *row 6, p53^{R175H}* mutant 1, and *row 7, p53^{R273H}* mutant 2). Interestingly, both *p53^{MT}* forms along with HO-3867 treatment resulted in a significant reduction in the volumes of the *p53$^{-/-}$* tumors (Fig. 3, *a and b*). It is important to note that HO-3867 treatment reduced the growth of both the *p53^{MT}* and the *p53^{null}* tumors because of the ability of the drug to become activated in the redox environments of these tumors (Fig. S1),

resulting in reactive oxygen species (ROS)-assisted death of tumor cells in *p53^{WT}* and *p53^{null}* tumors (51–54).

Because NMR data showed that HO-3867 covalently modified p53^{MT} at its DBD, it was essential to determine whether such interaction would result in the reactivation of p53-mediated transcription and up-regulation of p53 downstream genes. We prepared a panel of 29 cell lines carrying various mutations in the *p53* DBD (Fig. 4a). The p53 mutations of each of the 29 *p53^{MT}* cell lines are shown in Fig. 4a and Fig. S2. A digital quantitative real-time PCR (qPCR) analysis using the Fluidigm platform was performed in the 29 *p53^{MT}* cell lines to evaluate the expression of 14 genes with well-characterized p53 binding sites (55) (Figs. S3 and S4). The experiment was performed in control (untreated), HO-3867–treated (10 μM), HO-3867 plus p53 shRNA–treated, and cisplatin-treated cells (Fig. 4b). The *color blocks* (Fig. 4b) are arranged in order of the cell lines listed (Fig. 4a) by their respective p53 DBD mutations from N-to-C terminus. The expression of 14 p53-regulated genes was poor to average in untreated *p53^{MT}* cells (Fig. 4b, *red* to *yellow* color coding). The expression of these 14 genes was significantly increased in *p53^{MT}* cells upon treatment with HO-3867 (Fig. 4b, *blue* color coding). The HO-3867–induced increase in the expression of these 14 genes was reversed upon *p53* knockdown using lentivirus-based shRNA. Cisplatin treatment, which is used as standard care of therapy, did not activate p53-regulated genes in *p53^{MT}* cell lines (Fig. 4b). These data also suggest that the HO-3867–induced activation of p53-regulated genes in *p53^{MT}* lines was a specific biological effect not induced by other anticancer drugs such as cisplatin. It is important to recognize that other p53 reactivation drugs can target a specific set of p53 mutations (37–40, 43–45, 47–49); however, the biological activity of HO-3867 appeared to reactivate the transcriptional response of cells with an especially wide variety of p53 mutations as noted in (Figs. 4a and S2).

Because HO-3867 treatment resulted in increased expression of p53-regulated genes in *p53^{MT}* cells, we investigated whether this effect was associated with a direct interaction between p53^{MT} and p53-DBD at the promoter of the target genes. To further evaluate this possibility in a genetically tractable model, we conducted ChIP analysis in HO-3867–treated (10 μM) *p53^{MT}* (A-431) and *p53$^{-/-}$* (MCF-7 *p53$^{-/-}$*) cancer

Figure 1. HO-3867 exhibits differential cytotoxicity to cancer cells with *p53^{MT}* compared with healthy (noncancerous) cells. *a*, clinically relevant models were used to analyze the safety of HO-3867 toward normal body cells while simultaneously observing its anticancer efficiency in human cancer-derived cell populations. The graphical representation shows the isolation of heterogeneous cell populations from breast, colon, and liver cancer samples. In addition, noncancerous healthy cells such as fibroblasts from stromal tissue adjacent to breast cancer and radio- and chemosensitive cells from lymphoid and GI tract tissue were used. All of these cells were treated with HO-3867, cisplatin, or vehicle alone. *b*, a cancer-specific pro-apoptotic effect of HO-3867 was observed in all cells depicted in *panel a*. Cells were treated with HO-3867 (10 μM), cisplatin (10 μM), or vehicle (DMSO) alone, and apoptosis was measured using annexin V flow cytometry. HO-3867 selectively induced apoptosis in tumor-derived cells and minimal apoptosis in primary culture from normal tissue of different origins as well as tumor-adjacent stroma-derived fibroblasts and radiosensitive lymphoid and GI tract tissue. Cisplatin nonspecifically killed a significantly higher percentage of cells derived from normal tissues ($n = 3$ for all experiments; p values are as indicated, ANOVA was used for p value calculations, and *error bars* indicate standard deviation). *c*, *p53* mutational analysis of breast, colon, and liver cancer samples used for the cell cultures shown in *b* confirms the presence of DNA-binding domain mutations. The exact nucleotide sequence point mutations and resulting amino acid sequence changes are depicted. *d*, the ability of HO-3867 to induce apoptosis in cancer cells with a *p53^{MT}* genotype was determined using annexin V flow cytometry. *p53^{MT}* cells (A431, MDA-MB-468, WRO, and DU-145) and *p53$^{-/-}$* cells (MCF-7$^{p53-/-}$ and HCT7$^{p53-/-}$) were used in the analysis. Cellular apoptosis was not observed in untreated *p53^{MT}* and *p53$^{-/-}$* cells (*bars 1–6*). shRNA-mediated *p53* knockdown and the exogenous addition of *p53^{MT}* cDNA were used as controls in untreated cells (*bars 7–18*). In the experimental set, all cell lines were treated with HO-3867, and *p53^{MT}* cells showed a significant increase in cellular apoptosis (*bars 19–22*). HO-3867–treated *p53^{null}* cells did not show a marked increase in apoptosis (*bars 23–24*). shRNA-mediated *p53^{MT}* knockdown abolished the HO-3867–induced increase in apoptosis (*bars 25–30*). The exogenous addition of *p53^{MT}* cDNA alongside HO-3867 treatment significantly increased apoptosis in both *p53^{MT}* and *p53$^{-/-}$* cells (*bars 31–36*) ($n = 3$; mean $\pm$ S.D. shown). p values are shown on the figure; standard ANOVA test). *Inset*, the efficiency of lentiviral particles coding for *p53^{MT}* cDNA or *p53* shRNA was demonstrated using immunoblotting of MCF-7 *p53$^{-/-}$* or MCF-7 cells. Untreated MCF-7 *p53$^{-/-}$* samples showed no expression of *p53* (*lane 1*). Overexpression of increasing amounts of *p53^{MT}* cDNA led to increased p53 protein levels. *p53* shRNA treatment showed effective knockdown of p53 expression (a representative image from $n = 3$ replicates is shown).
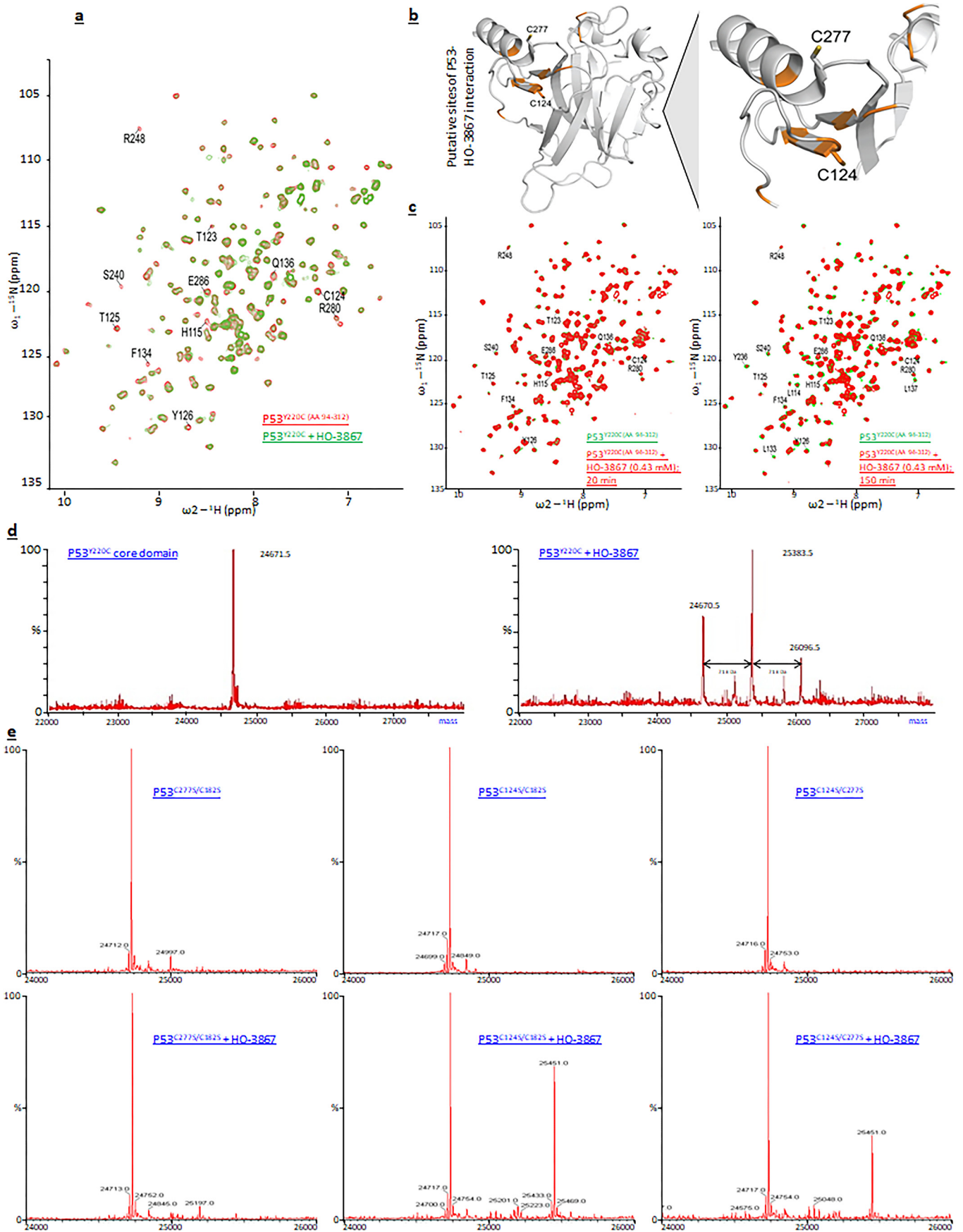
cells to assess the interaction of p53 with response elements (RE) of its critical apoptosis and cell-cycle regulatory genes *BAX* and *CIP1 (*p21 gene), respectively (Fig. 4c). HO-3867 treatment resulted in a significant increase in p53–RE interaction in $p53^{MT}$ cells, which was reversed upon *p53* silencing. Further, no p53–RE interaction was observed in $p53^{-/-}$ cells. However, the restoration of p53–RE interaction was observed in HO-3867–treated $p53^{-/-}$ cells exogenously expressing $p53^{MT}$, suggesting that HO-3867 can directly restore the binding of $p53^{MT}$ chromatin interaction. The results were further corroborated at the protein level by performing a Western blotting for two crucial p53 downstream targets, p21 and NOXA (Fig. 4d). $p53^{WT}$ (MCF-7), $p53^{MT}$ (A-431), and $p53^{-/-}$ (MCF-7 $p53^{p53-/-}$) cancer cells were used for the study. HO-3867 treatment resulted in an increase in protein expression in both $p53^{WT}$ and $p53^{MT}$ cancer cells (Fig. 4d, *lanes 4* and *5*) compared with untreated control cells (*lanes 1–3*). Further, the treatment showed no effect on the $p53^{-/-}$ cancer cells (Fig. 4d, *lane 6*). A significant increase in NOXA and p21 expression was observed in HO-3867–treated $p53^{-/-}$ cells, exogenously expressing $p53^{MT}$ cDNA (Fig. 4d, *lane 8*) compared with untreated $p53^{-/-}$ cells exogenously expressing $p53^{MT}$ cDNA alone (*lane 7*). These findings substantiate the role of HO-3867 in the restoration of $p53^{WT}$ transcriptional activity.

Next, we sought to identify the mechanistic changes that enable p53^{MT} to interact with chromatin in the presence of HO-3867. The p53 conformation-specific antibodies (Ab) 1620 and 240 were used to specifically detect cellular p53^{WT} and p53^{MT} forms, respectively (56). Immunoprecipitation assays using Ab 1620 and Ab 240 with lysates from A-431 ($p53^{MT}$), MCF-7 ($p53^{WT}$), and MCF-7 $p53^{-/-}$ tumors were performed to determine whether HO-3867 induces a p53^{MT} to p53^{WT} conformational change in $p53^{MT}$ tumors and cell lines (Fig. 5a). In untreated MCF-7 tumors, p53 was recognized by Ab 1620 (*lane 3*), and a small fraction of cellular p53 was also recognized by Ab 240. This observation is consistent with previous studies, as some fraction of p53 in wildtype cells or tissues exists in a misfolded/unfolded form, which is recognized by the p53^{MT}-specific Ab 240 (32, 56). In untreated A-431 tumors, p53 was recognized by Ab 240 (Fig. 5a, *lane 4*). However, HO-3867-treatment (20 mg/kg) of A-431 tumors resulted in the conversion of p53 conformation from an Ab 240–recognized to an Ab 1620–recognized form (Fig. 5a, compare *lane 4* with *lane 11*). The exogenous addition of $p53^{MT}$ cDNA in HO-3867–treated A-431, MCF-7, and MCF-7 $p53^{-/-}$ tumors showed a strong presence of p53 in a wildtype form recognized by Ab 1620 (Fig. 5a, compare *lanes 9* and *10* with *lanes 17* and *18*). Similar experiments using Ab 1620 and Ab 240 were repeated in MCF-7, HCT ($p53^{WT}$), A-431, DU-145, MDA-MB-231 ($p53^{MT}$), and MCF-7 $p53^{-/-}$, HCT $p53^{-/-}$ cell lines (Fig. 5b). In untreated

$p53^{MT}$ cells, p53^{MT} existed exclusively in a mutant form recognized by Ab 240 (Fig. 5b, *rows 5–7, lane 4*). Upon HO-3867 treatment (10 μM) of $p53^{MT}$ cells, p53^{MT} is converted to a wild-type form recognized by 1620 Ab (compare conversion from 240 to 1620 form) (Fig. 5b, *lanes 4* and *5*). Together, these data suggest that HO-3867 treatment in $p53^{MT}$ xenografts and cell lines converted p53 from a mutant to a wildtype conformation.

Using an *in vitro* cell-free transcription assay with a synthetic DNA template, we further analyzed whether the HO-3867–induced change in p53^{MT} conformation to the wildtype form would also result in the activation of p53^{MT}-dependent transcription. The DNA template pWAFMLT consisted of a poly(6)-p53 DNA-binding site (*p21*-DBS) followed by an adenovirus major late core promoter (AdMLT), a transcription start site, a G-less cassette as the coding region, and a poly(A) tail coding region (for qPCR-based detection) followed by a CCT stop signal respective to the G-less cassette (57) (Fig. 5c, *top*). The *in vitro* transcription assay was designed where nuclear extracts from $p53^{-/-}$ H1299 cells were the only source of RNA polymerase machinery. p53 immunoprecipitated from HO-3867–treated (10 μM) and untreated MCF-7 ($p53^{WT}$), A-431, T47D, MDA-MB-468, and DU-145 cell lines was used to observe p53^{MT}-dependent *in vitro* transcription. p53 immunoprecipitated from HO-3867–treated cells significantly increased *in vitro* transcript synthesis when incubated with H1299 nuclear extracts (Fig. 5c, *bottom*). These results were further confirmed via a luciferase-based reporter transcription assay under *in vivo* conditions using the same set of $p53^{MT}$, $p53^{WT}$, and $p53^{-/-}$ cell lines. In accordance with the *in vitro* transcription assay, the luciferase assay showed HO-3867–induced transcription by p53^{MT} in multiple cell types (Fig. 5d). These results document the ability of HO-3867 to modulate p53^{MT} activity by changing its conformation and directly restoring p53 transcriptional activity.

p53 is one of the most frequently mutated genes in cancer, and $p53^{MT}$ promotes aggressive oncogenic phenotypes. Thus, restoration of $p53^{WT}$ function is actively being explored as an anticancer strategy and p53 reactivation drugs have an important role. Clinical use of this class of drugs has been precluded because of their non-specificity and cytotoxicity. In this study, we demonstrated the anticancer properties of HO-3867, which induced apoptosis in cancer cells with minimal toxicity to normal cells. Mechanistically, HO-3867 covalently bound to mutant p53 and restored its wildtype conformation, transcriptional activity, and anticancer function. Gain of wildtype-like p53 function upon HO-3867 treatment effectively blocked cancer growth in mouse models, irrespective of *p53* mutational status. Importantly, HO-3867 restored the wildtype activity of a variety of p53 DBD mutants, which makes it a suitable drug for targeting cancers with complex p53 mutational status. Taken

Figure 2. HO-3867 covalently binds to p53^{MT} in the DNA-binding domain. *a,* ^{1}H-^{15}N HSQC NMR spectrum of the p53^{MT}-Y220C core domain (75 μM) after incubation with (*green*) or without (*red*) 1000 μM HO-3867 for 70 min. Chemical shift perturbations were observed for residues in proximity to the solvent-exposed cysteine 277. *b,* an NMR-generated model depicting the putative sites of interaction between p53^{MT} and HO-3867. *c,* ^{1}H-^{15}N-HSQC NMR spectrum of the p53^{MT}-Y220C core domain (75 μM) after incubating with (*green*) or without (*red*) 430 μM HO-3867 for 20 or 150 min. Chemical shift perturbations were time-dependent, suggesting a covalent binding mode. *d,* ESI (ES+) mass spectra of the p53^{MT}-Y220C core domain (50 μM) after incubation without (*left*) or with HO-3867 (*right*) for 4 h at room temperature. HO-3867 treatment led to a mass increase of 713 or 1426 Da, confirming covalent binding to the p53 core domain by HO-3867. *e,* ESI (ES+) mass spectra of p53 DBD (50 μM) C182S/C277S, C124S/C277S, and C124S/C182S mutants after incubation without (*left*) or with HO-3867 (*right*) for 4 h at room temperature. HO-3867 treatment led to a mass increase of 713 Da only for the C124S/C277S and C124S/C182S mutants, confirming selective covalent modification of Cys-277 and Cys-182 by HO-3867.
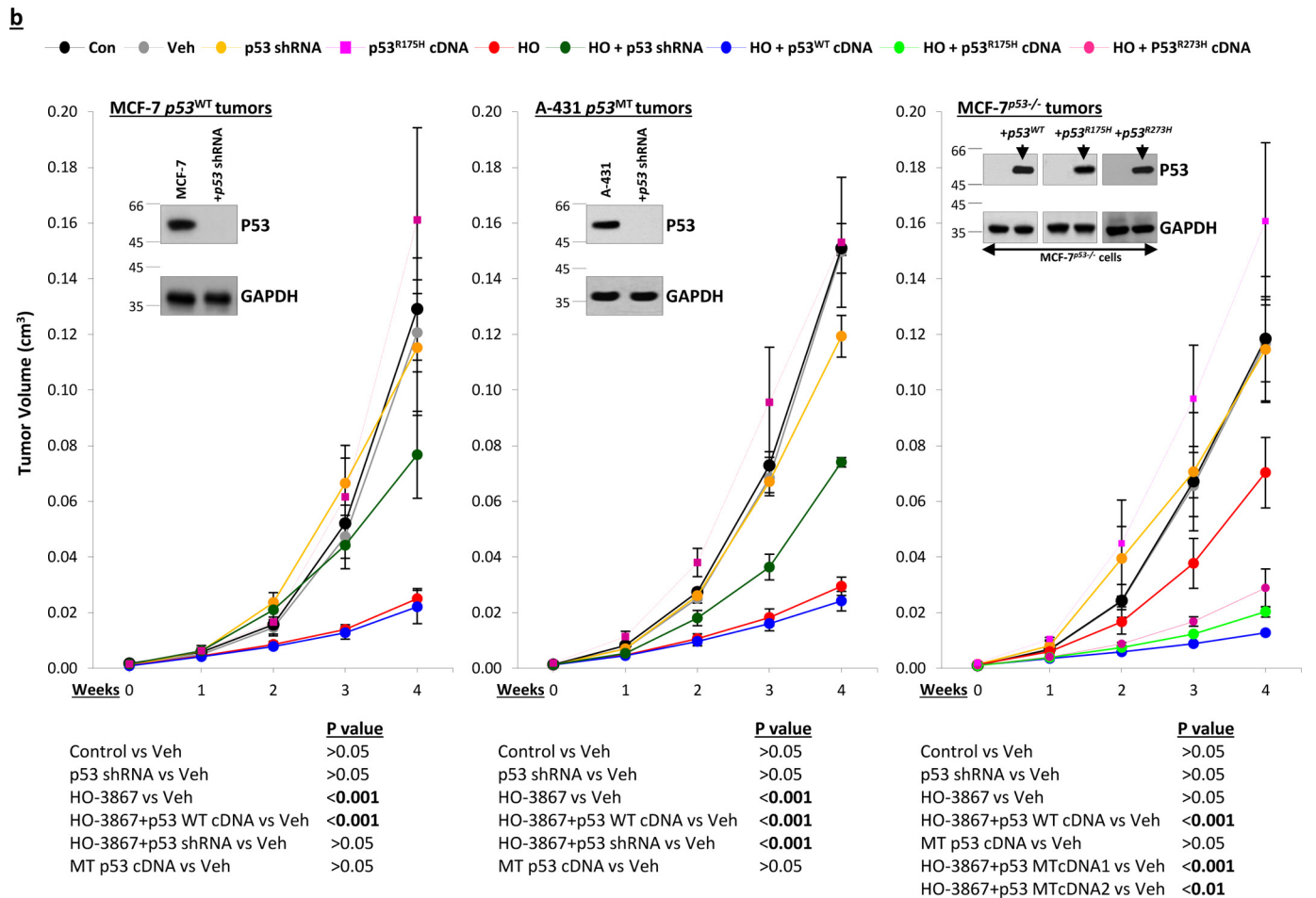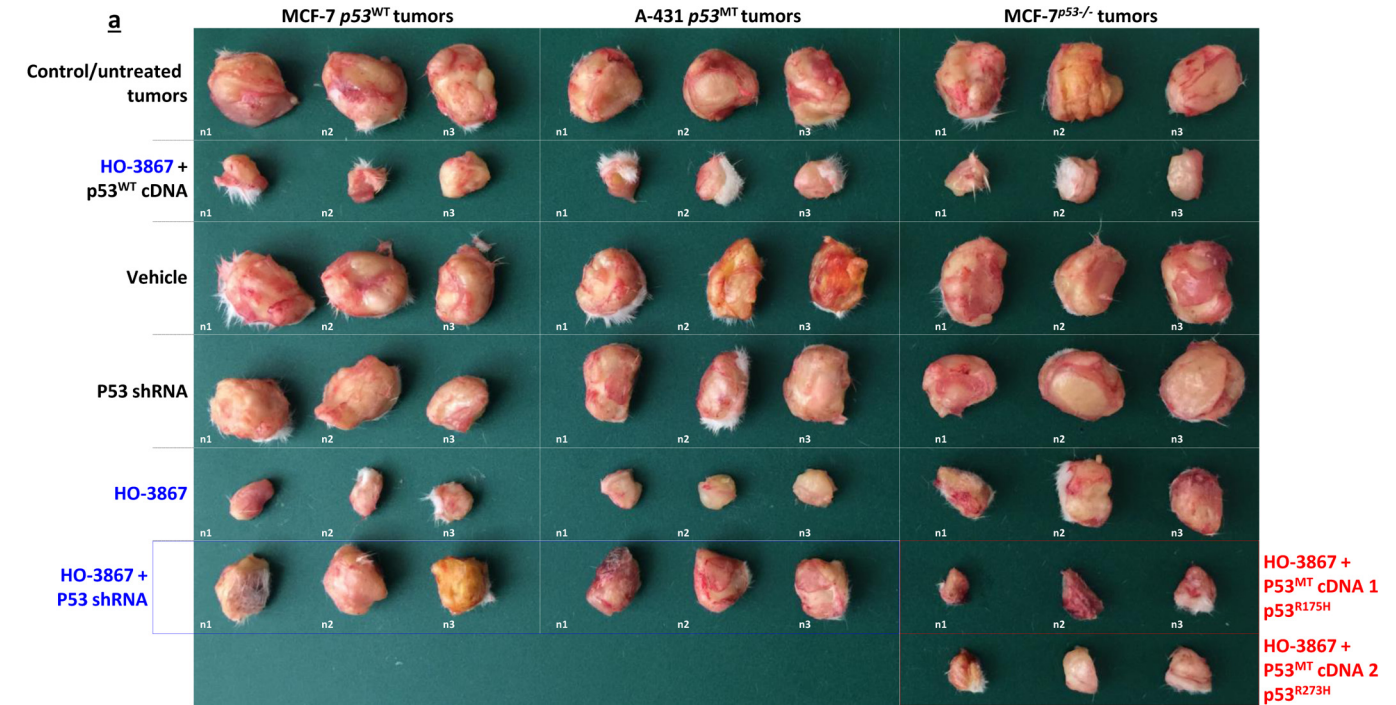
together these results highlight the potential of HO-3867 as a safe, specific, and effective anticancer drug.

Experimental procedures

Cell lines and culture conditions

$p53^{MT}$ cells (HEC-1-A, CCRF-CEM, KLE, T47D, SW837, MDA-MB-468, SK-UT-1, SK-LMS-1, SKLU1, Calu-6, SNU-16, DMS-53, SW1271, BT-20, BT-549, MDA-MB-231, BT-474, HOS, DLD-1, MOLT-4, WiDr, PSN-1, MC116, ST486, P3HR-1, NCI-H23, HT-3, NCI-H1882, WRO, HCT-15, A-431, and DU-145), $p53^{WT}$ (MCF-7 and HCT116), and 293T cells (for lentiviral production) were procured from ATCC (Manassas, VA). $p53^{-/-}$ cells were derived from $p53^{WT}$ (MCF-7 and HCT116) as described previously (9). Normal breast fibroblasts were isolated at Barts Cancer Institute, Queen Mary University of London, using surgically resected breast tissue with Dulbecco's modified Eagle's medium (DMEM)/F12 + 10% fetal bovine serum (FBS), penicillin/streptomycin, and 2.5 μg/ml Fungizone. Tumor cell populations from breast, colon, and liver cancer tissue and normal cells from lymphoid and GI tract tissue were extracted using human tissue material provided by United Kingdom-based Tissue for Research, as described previously (58). Briefly, the cells were cultured in monolayer in respective growth media (DMEM or RPMI 1640) supplemented with 10% (v/v) heat-inactivated FBS and antibiotics (1% penicillin/streptomycin) and incubated at 37 °C in a humidified atmosphere of 95% air and 5% CO_2.

NMR

^{1}H-^{15}N HSQC sample spectra were recorded and analyzed as described (59). Briefly, samples containing uniformly ^{15}N-labeled T-p53C-Y220C (75 μM) and 0.43 or 1 mM HO-3867 were measured at 293 K on a Bruker Avance-800 spectrometer using a 5-mm inverse cryogenic probe after 20, 70, or 150 min of incubation at room temperature. Spectral analysis was performed using Sparky 3.11430 and Bruker Topspin 2.0 software. A previously described assignment map of the p53-Y220C DBD was used to label residues (60).

Mass spectrometry

Samples containing 50 μM T-p53C-Y220C (residues 94-312) or 50 μM T-p53C (residues 94–312) cysteine to serine mutants (C277S/C182S, C277S/C124S, and C182S/C124S), 25 mM potassium phosphate, pH 7.2, 150 mM sodium chloride, 1 mM tris(2-carboxyethyl)phosphine, and 5% DMSO were prepared with or without 2 mM HO-3867 and incubated for 4 h at 20 °C. The samples were then diluted to 5 μM protein in 100 mM ammonium acetate buffer and desalted using Millipore C4 Zip-Tips. Protein mass was determined via electrospray mass spectrometry with a Waters (Milford, MA) Micromass LCT TOF mass spectrometer in ESI (ES+) mode.

Digital droplet qPCR

Digital droplet qPCR was performed at the University of Nebraska DNA Sequencing Core (Omaha, NE). Reverse transcription, preamplification, and qPCR were performed according to the manufacturer's protocols (Fluidigm, San Francisco, CA). cDNA preparation was performed with 100 ng of RNA using Fluidigm RT master mix. Reverse transcription was followed by 10 preamplification cycles, cleanup with Exonuclease I (Fluidigm), and then a 10-fold dilution. qPCR was performed for 30 cycles.

Chemicals, kits, and plasmids

DMEM, RPMI, penicillin, streptomycin, FBS, trypsin-EDTA, PBS, TRIzol reagent, Lipofectamine 2000 transfection reagent, Dynabeads-protein A, the SuperScript® VILO™ cDNA synthesis kit, and other chemicals of culture grade were purchased from Life Technologies. Dichlorofluorescin diacetate and DMSO were procured from Sigma. Protein G PLUS-agarose was procured from Santa Cruz Biotechnology Inc. (Santa Cruz, CA). Calibrated pipettes used for EPR were procured from VWR International. An annexin V FITC detection kit and a 1:1 mixture of Matrigel were obtained from BD Biosciences. A Cignal p53 Reporter (luciferase) kit was purchased from Qiagen. Anti-rabbit p53 (FL-393) polyclonal antibodies; anti-mouse p53 WT conformation 1620 and p53 MT conformation 240 monoclonal antibodies; and goat anti-rabbit IgG-HRP and anti-mouse IgG-HRP secondary antibodies (Santa Cruz Biotechnology) were used. $p53^{WT}$, $p53^{MT\ R175H}$, $p53^{MT\ R273H}$, and $p53^{MT\ Y220C}$ plasmids were procured from Addgene (Cambridge, MA).

Figure 3. HO-3867 shows anticancer efficacy in both p53^{MT} and p53^{WT} tumor xenografts by inducing p53^{MT}–RE interaction and induces expression of p53 downstream effectors. *a*, the anticancer effect of HO-3867 on genetically tractable tumor xenografts of $p53^{WT}$ (MCF-7), $p53^{MT}$ (A-431), and $p53^{-/-}$ (MCF7 p53$^{-/-}$) cells was observed ($n = 3$). In *row 1*, the excised tumors for untreated $p53^{WT}$, $p53^{MT}$, and $p53^{-/-}$ xenografts after 4 weeks are shown. In *row 2*, all of the tumors were treated with HO-3867 along with lentivirus-assisted overexpression of p53^{WT}. A reduction in the tumor volumes of all tumor types was observed in *row 2* when compared with the control (*row 1*). In *row 3*, tumors were treated with vehicle (DMSO) and lentiviral transfections. The tumor volumes in the vehicle-treated group remained unaltered. In *row 4*, all tumors were treated with lentivirus coding for p53 shRNA. In *row 5*, all tumors were treated with HO-3867, and $p53^{WT}$ tumors and $p53^{MT}$ tumors showed a decrease in tumor volume for all biological replicates. Interestingly, in *p53* knockdown tumors, HO-3867 did not exhibit very high anticancer efficacy. These data suggest a role for p53 in HO-3867-mediated anticancer activity that appears to be independent of p53 mutational status. In *row 6*, $p53^{WT}$ and $p53^{MT}$ tumors were treated with HO-3867 along with lentiviral particles coding for p53 shRNA. p53 knockdown in these tumors reversed the anticancer effect of HO-3867, and all biological replicates in both experimental groups showed larger tumor volumes. In *rows 6 and 7*, *p53* null tumor xenografts were treated with HO-3867 and lentiviral particles coding for $p53^{MT}$ cDNA (p53^{R175H} (*row 6*); p53^{R273H} (*row 7*)). Interestingly, HO-3867 reduced tumor growth in the presence of $p53^{MT}$ cDNA (compare tumor volumes in *row 5* with *rows 6 and 7*) ($n = 3$) (HO-3867 treatment started at week 0 in the plot). *b*, tumor growth curves showing the volume of MCF-7 $p53^{WT}$, A-431 $p53^{MT}$, and MCF-7 $p53^{-/-}$ tumors in the eight treatment groups over the course of 4 weeks. In both MCF-7 $p53^{WT}$ and A-431 $p53^{MT}$ tumors, treatment with HO-3867 and HO-3867+ $p53^{WT}$ cDNA led to the greatest reduction in tumor volume. Treatment of MCF-7 $p53^{-/-}$ tumors with HO-3867, HO-3867+$p53^{R175H}$ cDNA, and HO-3867+$p53^{R273H}$ cDNA led to a significant reduction in tumor volume compared with control. In the *insets*, the efficiency of lentiviral particles coding for p53 shRNA, $p53^{WT}$ cDNA, or $p53^{MT}$ cDNA was demonstrated in MCF-7 $p53^{WT}$ or A-431 $p53^{MT}$ cells using immunoblotting with the indicated antibodies. MCF-7 $p53^{WT}$ and A-431 $p53^{MT}$ samples treated with *p53* shRNA showed no expression of *p53* (*lane 2*). p53 shRNA showed effective knockdown of p53 expression. MCF-7 $p53^{-/-}$ cells were treated with $p53^{WT}$, $p53^{R175H}$, and $p53^{R273H}$ cDNA and blotted with anti-p53 antibody or anti-GAPDH antibody (loading control). Overexpression of $p53^{WT}$ cDNA or $p53^{MT}$ cDNA led to increased p53 protein expression in MCF-7 $p53^{-/-}$ cells (HO-3867 treatment started at week 0 in the plot). $n = 3$ for all experiments; p values are labeled on the figure, and two-factor ANOVA with repeated measures was performed for p value calculations.

![ASBMB]

J. Biol. Chem. (2018) 293(12) 4262–4276 **4269**
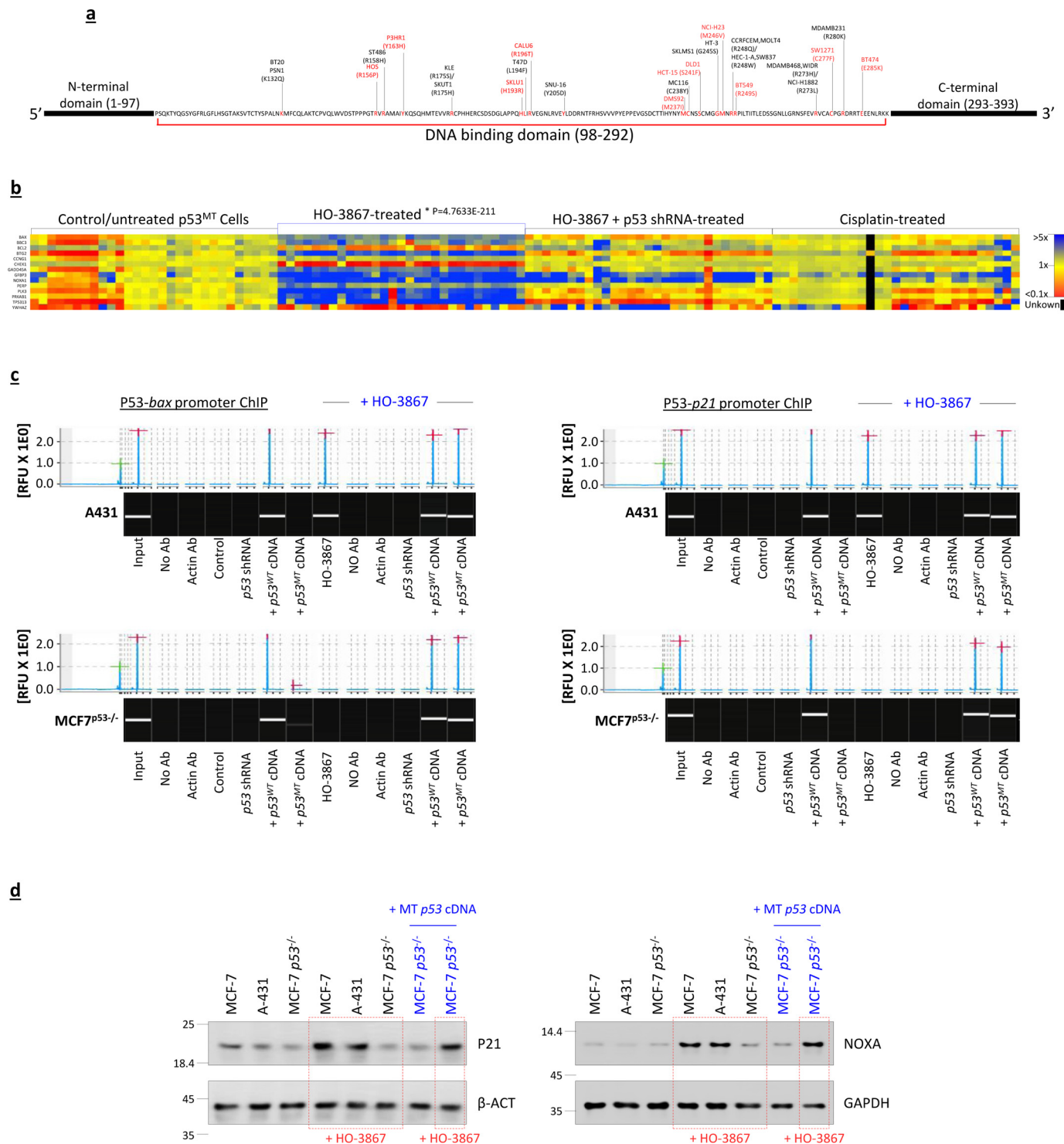
Figure 4. HO-3867 converts mutant p53 conformation to its wildtype form. *a*, model depicting sites of mutagenesis in the *p53* gene in a panel of 29 cell lines. All mutations are present in the *p53* DNA-binding domain. *b*, a Fluidigm digital qPCR-based gene expression analysis of a panel of 14 genes (Fig. S3) was conducted in a panel of 29 control and HO-3867–treated cell lines. Consistent with qChIP analysis, p53-regulated genes were overexpressed in all HO-3867–treated *p53^MT* cell lines; this effect was reversed upon *p53* shRNA treatment. Cisplatin (10 μM) was used as a positive control for p53 activation. (*n* = 5 for all experiments; *p* values are labeled on the figure, and ANOVA was performed for *p* value calculations). *c*, ChIP analysis was conducted in a genetically tractable system of *p53^MT* (A-431) and *p53^−/−* (MCF-7^p53−/−) cell lines to measure the binding of *p53^MT* to its REs at the *bax* (*left*) and *p21* (*right*) promoters. The results were analyzed using the QIAxcel advanced instrument platform (Qiagen). Input (*lane 1*), no antibody (*lane 2*), actin antibody (*lane 3*), and *p53* shRNA (*lanes 5 and 11*) were used as controls. The data show the presence of p53 on the *bax* and *p21* promoters in HO-3867–treated *p53^WT* and *p53^MT* cell lines but not *p53^−/−* cell lines (*lane 8*). Exogenous addition of either *p53^WT* (*lane 12*) or *p53^MT* (*lane 13*) cDNA resulted in significant binding of p53 at its respective REs in HO-3867–treated *p53^MT* and *p53^−/−* cell lines. *d*, up-regulation of two important p53 target genes, *p21* and *Noxa*, was confirmed at the protein level by Western blotting. A genetically tractable system of p53^WT (MCF-7), p53^MT (A-431), and p53^−/− (MCF-7 p53^−/−) cells was used to study the effect of HO-3867 treatment (10 μM) in p53^MT cells (*lanes 1–6*). *Lane 7*, both p21 and Noxa Western blotting show less expression in MCF-7 p53^−/− cells transfected with p53^MT cDNA. However, the same combination in the presence of HO-3867 significantly increases p21 and Noxa expression (*lane 8*).
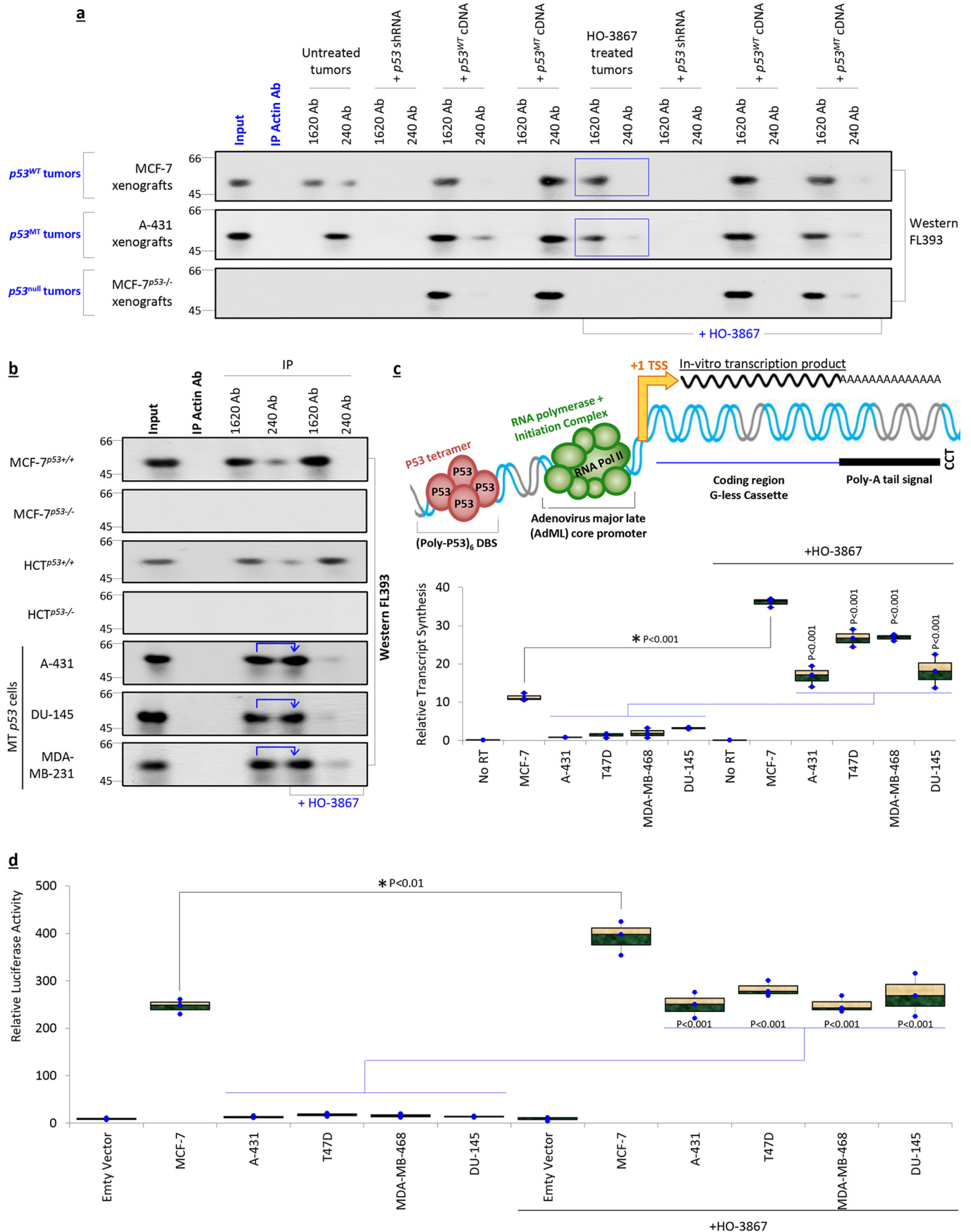
Protein expression and purification

The stabilized DNA-binding domain (residues 94–312) of the p53 mutant Y220C (T-p53C-Y220C) and T-p53C cysteine mutants (C124S/C277S, C124S/C182S, and C182S/C277S) were expressed and purified as described (60).

Treatment with HO-3867

All stock solutions for HO-3867 were freshly prepared in DMSO. HO-3867 (molecular mass, 713 Da) was synthesized and purified as described previously (49–51). For cell line–based studies, a dose of 10 μM concentration was used for treatment. For animal studies, mice were administered with HO-3867 (20 mg/kg body weight) in 0.2 ml intravenously. Injections were performed once daily for the first 7 days of treatment followed by one injection (20 mg/kg body weight) every 8 days until the end of the treatment schedule.

Gene silencing and overexpression using lentiviral transduction

All work with lentiviruses was performed under BL2/BSL-2 conditions. Lentiviral particles were produced in 293T cells plated in a 96-well plate (20,000 cells/well) and supplemented with 10% fetal bovine serum and 4 mM L-glutamine 24 h prior to infection. For the knockdown of both WT and MT *p53*, the cells were co-transfected with a combination of five different MISSION *p53* shRNA particles (SHCLNG-NM_000546) (Sigma) along with a MISSION lentiviral packaging mix (Sigma) using Lipofectamine 2000 reagent (Sigma). For the overexpression of WT *p53* cDNA or MT *p53* cDNA, the ViraSafe™ (Pantropic) lentiviral packaging system (Cell Biolabs, San Diego, CA) was used to generate lentiviruses. The supernatant was collected starting at 24–72 h post-transfection, pooled, and filtered through a 0.45-μm filter. The virus particles were concentrated by ultracentrifugation, and the physical titer of virus particles was determined as per the manufacturer's protocol. For animal studies, lentiviral transduction of tumors *in vivo* was achieved in established cell line (A-431, MCF-7, and MCF-7 (p53$^{-/-}$))

xenografts. Briefly, once tumor sizes reached 1–1.5 cm^3, mice were anesthetized with 1.5–3% isoflurane with 30% oxygen, and *in vivo* transduction of the lentivirus was achieved through intratumoral injections of the desired lentivirus. Lentiviral supernatant was thawed at 37 °C and diluted in 0.9% saline (injection, USP) and Polybrene (4 μg/ml final concentration) to give a dose of 1.6 × 10^8 transduction units (TU) in a 50-μl volume/injection (intratumoral). Multiple injections per tumor were given to cover the spread of the lentivirus throughout the tumor volume. The respective lentiviral injections were given twice daily for the first 4 days of the treatment followed by once every 3 days until the end of the treatment. The viral supernatants were mixed with Lipofectamine 2000 (5% final v/v, Invitrogen) 30 min before the instillation to increase the transduction efficiency.

Cancer xenografts

Female athymic *nu/nu* mice were housed in laminar flow cabinets under specific pathogen-free conditions and used at 4–5 months of age. All animals were used when between 20–22 g in weight and were purchased from Taconic Biosciences. Food and water were available *ad libitum* for the duration of the studies. All animal protocols were approved by the Institutional Animal Care and Use Committee at Dartmouth College. The cell line xenografts were established as described previously (9, 11, 32). Briefly, the desired cell lines (A-431, MCF-7 (p53$^{+/+}$) and MCF-7 (p53$^{-/-}$)) were maintained in DMEM/F12 supplemented with 10% FBS and 1% antibiotics. For injection, cells at 70–90% confluency were trypsinized and resuspended in serum-free media with 1:1 Matrigel at a concentration of 1 × 10^7 cells/ml on ice. Cell viability, required to be at least >95%, was determined by a trypan blue exclusion assay. For tumor induction, animals were first anesthetized with 1.5–3% isoflurane with 30% oxygen. An 80-μl cell suspension containing 1 × 10^7 cells was subcutaneously injected in the left or right mammary gland of mice. The vehicle control used for the study was DMSO. Tumor volumes monitored weekly by caliper measure-

Figure 5. HO-3867 converts mutant p53 conformation to its wildtype form. *a*, the p53^{MT} and p53^{WT} forms were immunoprecipitated using Ab 240 or Ab 1620, respectively, and immunoblotted using a polyclonal anti-p53 antibody (FL393) in *p53^{MT}* (A-431), *p53^{WT}* (MCF-7), and MCF-7$^{p53-/-}$ tumors. Input (*lane 1*), actin antibody (*lane 2*), and *p53* shRNA (*lanes 5* and *6*) were used as controls for all tumors. In untreated MCF-7 tumors, p53 was recognized by Ab 1620 (*lane 3*) and to a minor extent by Ab 240 (*lane 4*). In untreated A-431 tumors, p53 was exclusively recognized by Ab 240 (*lane 4*). No signal was detected in MCF-7$^{p53-/-}$ tumors (*third row*). Overexpression of *p53^{WT}* and *p53^{MT}* cDNA in all three tumors resulted in a strong signal for Ab 1620 (*lane 7*) and Ab 240 (*lane 10*), respectively. HO-3867 treatment in MCF-7 tumors significantly increased detection by Ab 1620 (compare *lanes 3* with *11*). HO-3867 treatment in A-431 tumors resulted in a change in the p53 conformation from an Ab 1620–recognized form to an Ab 1620–recognized form (compare *lanes 4* and *11*). HO-3867 had no effect on MCF-7$^{p53-/-}$ tumors. Exogenous addition of *p53^{WT}* cDNA in HO-3867–treated A-431, MCF-7, and MCF-7$^{p53-/-}$ tumors showed the strong presence of p53 in the Ab 1620–recognized form (*lanes 15* and *16*). Exogenous addition of *p53^{MT}* cDNA in HO-3867–treated A-431, MCF-7, and MCF-7$^{p53-/-}$ tumors again showed the strong presence of p53 in the Ab 1620–recognized form (*lanes 17* and *18*) (*n* = 3). *b*, wildtype and mutant forms of p53 were immunoprecipitated using Ab 1620 and Ab 240, respectively, and immunoblotted for p53 protein (FL393) in *p53^{WT}* (MCF-7 and HCT) or *p53^{MT}* (A-431, DU-145, and MDA-MB-231) cell lines. Input (*lane 1*) and actin antibody (*lane 2*) were used as controls. In untreated *p53^{WT}* cells, p53 was recognized by Ab 1620 (*lane 3, rows 1* and *3*). p53$^{-/-}$ (MCF-7$^{p53-/-}$ and HCT$^{p53-/-}$) cells served as negative controls and showed no p53 signal (*rows 2* and *4*). In untreated *p53^{MT}* cells, p53 existed exclusively in an Ab 240–recognized form (*lane 4, rows 5–7*), which upon HO-3867 treatment converted to an Ab 1620–recognized form (compare conversion from 240 to 1620 form, *lanes 4* and *5*) (*n* = 3). *c*, graphical representation of the experimental design for conducting *in vitro* transcription assays (*top*). The synthetic DNA template consisted of a poly(6)-p53 DNA-binding site followed by an adenovirus major late core promoter, a transcription start site, a G-less cassette as the coding region, and a poly(A) tail coding region (for qPCR-based detection) followed by a CCT stop signal. Nuclear extracts from *p53^{null}* (H1299) cells were the source of the RNA polymerase machinery. Lack of reverse transcriptase to convert synthetic transcripts to a qPCR-detectable form in the reaction mix served as a negative control (*No RT, bars 1* and *7*). p53 immunoprecipitated from untreated MCF-7 cells in combination with H1299 nuclear extracts showed basal transcript synthesis (*second bar*). p53 from *p53^{MT}* cell lines in combination with H1299 nuclear extract resulted in minimal transcript synthesis (*bars 3–6*). p53 immunoprecipitated from HO-3867–treated *p53^{WT}* and *p53^{MT}* cell lines in combination with H1299 nuclear extracts successfully generated RNA transcripts from the synthetic DNA template (*blue*) (*n* = 3 for all experiments; *p* values are labeled on the figure, and ANOVA was performed for *p* value calculations). *d*, luciferase-based reporter transcription assay (Cignal) was used to analyze p53-dependent transcription in HO-3867–treated *p53^{MT}* cell lines *in vivo*. Empty vector (*bars 1* and *7*) was used as a negative control. Standard p53-dependent transcription was observed in *p53^{WT}* MCF-7 cells. Results showed minimal p53-dependent transcription in a variety of *p53^{MT}* cell lines. The effect of HO-3867 on p53-induced transcription was observed in treated *p53^{WT}* and *p53^{MT}* cells (*n* = 3 for all experiments; *p* values are labeled on the figure, and ANOVA was performed for *p* value calculations).

ment of the length, width, and height were calculated using the formula for a semi-ellipsoid ((L*L*W)/2). After 3 weeks, mice bearing tumors with volumes averaging ~0.0015 cm^3 were randomized for treatments in different groups (3 mice/group).

Annexin V flow cytometry

A Becton Dickinson flow cytometer (BD-LSR II, BD Biosciences) was used to detect the apoptotic cell surface shift of phosphatidylserine by the binding of FITC-conjugated annexin V to the outer membrane of intact cells. The attached cells (untreated and treated (24 h)) were gently scraped off the dish, centrifuged (500 × g for 5 min), and washed in PBS (Ca^{2+}- or Mg^{2+}-free), 0.1% EDTA. The pelleted cells were treated with 500 μl of binding buffer followed by 5 μl of FITC, and then 5 μl of propidium iodide (10 μg ml^{-1}) was added. Cells were incubated at room temperature for 5 min. These cells were then filtered (70-μm mesh) to eliminate cell aggregates and analyzed by flow cytometry.

Luciferase assay

To study the effect of HO-3867 on transcription by p53^{MT}, the p53^{MT} cells were plated in 35-mm Petri dishes the day before transfection so that they could reach 60–80% confluency upon transfection. Reporter plasmids (1.0–1.5 mg/well) were transfected with Lipofectamine 2000 reagent as per the manufacturer's instructions. After the desired incubation period, the cells (untreated and treated (24 h)) were washed in cold PBS three times and lysed with 200 μl of the lysis buffer by a freeze-thaw cycle, and the lysates were collected by centrifugation at 14,000 rpm for 2 min in a benchtop centrifuge. 20 μl of supernatant was used for the assay of luciferase activity using a Cignal p53 Reporter (luc) kit as per the manufacturer's instructions.

Chromatin immunoprecipitation

The ChIP experiments were performed essentially as described previously (9, 31, 61, 62). An anti-p53 (FL-393) rabbit polyclonal antibody was used for the study. Formaldehyde was added at a final concentration of 1% directly to the cell culture media. Fixation proceeded at 22 °C for 10 min and was stopped by the addition of glycine to a final concentration of 0.125 M. The cells (untreated and treated (24 h)) were collected by centrifugation and rinsed in cold phosphate-buffered saline. The cell pellets were resuspended in swelling buffer (10 mM potassium acetate, 15 mM magnesium acetate, 0.1 M Tris, pH 7.6, 0.5 mM phenylmethylsulfonyl fluoride, and 100 ng of leupeptin and protinin/ml), incubated on ice for 20 min, and then Douncehomogenized. The nuclei were collected by microcentrifugation and then resuspended in sonication buffer (1% SDS, 10 mM EDTA, 50 mM Tris-HCl, pH 8.1, 0.5 mM phenylmethylsulfonyl fluoride, and 100 ng of leupeptin and aprotinin/ml) and incubated on ice for 10 min. Prior to sonication, 0.1 g of glass beads (212- to 300-mm diameter, Sigma) was added to each sample. The samples were sonicated on ice with an Ultrasonics sonicator at setting 10 for six 20-s pulses to an average length of ~1,000 bp and then microcentrifuged. The chromatin solution was precleared with the addition of *Staphylococcus aureus* protein A–positive cells. Prior to the first wash, 20% of the super-

natant from the reaction with no primary antibody for each time point was saved as total input chromatin and was processed with the eluted immunoprecipitates beginning at the cross-link reversal step. Cross-links were reversed by the addition of NaCl to a final concentration of 200 mM, and RNA was removed by the addition of 10 mg of RNase A/sample followed by incubation at 65 °C for 4–5 h. The samples were then precipitated at 20 °C overnight by the addition of 2.5 volumes of ethanol and then pelleted by microcentrifugation. The samples were resuspended in 100 ml of Tris-EDTA, pH 7.5, 25 ml of proteinase K buffer (1.25% SDS, 50 mM Tris, pH 7.5, and 25 mM EDTA), and 1.5 ml of proteinase K (Roche Applied Science) and incubated at 45 °C for 2 h. After digestion with proteinase K, samples were extracted with phenol-chloroform-isoamyl alcohol (25:24:1) and then precipitated with 1/10 volume of 3 M sodium acetate NaOAc, pH 5.3, 5 mg of glycogen, and 2.5 volumes of ethanol. The pelleted chromatin was collected by microcentrifugation, resuspended in 30 μl of water, and analyzed by PCR and qPCR to study p53–RE interaction at the promoter of *bax* or *p21* genes. The primers used for ChIP analysis are as described previously (55).

The samples were run on the QIAxcel Advanced instrument (Qiagen) using a QIAxcel DNA high resolution kit (Qiagen) and the 0M500 method (sample injection voltage of 5 kV and separation voltage of 5 kV) with a sample injection time of 15 s. During the run we used the QX DNA Size Marker, 25–500 bp, version 2.0, and the corresponding QX Alignment Marker, 15/600 bp (Qiagen). To analyze the results, we used QIAxcel ScreenGel software. Sample analyses were performed using a two-step approach. First, peaks were detected in the raw data. In a second step, the peak sizes and peak concentrations were determined by mapping the detected peaks to the peaks of the reference size marker.

Reverse-transcriptase real-time PCR

Using the TRIzol method, RNA was extracted from cells and tumor grafts following transfections with respective cDNAs and treatment with HO-3867 (24 h). cDNAs were synthesized from 2.5 μg of RNA in a 20-μl volume using the SuperScript VILO cDNA synthesis kit (Thermo Fisher Scientific) according to the manufacturer's protocol. qPCR was performed using 384-well plates in a final volume of 20 μl on QuantStudio 6 Flex (Applied Biosystems, Life Technologies). TaqMan Universal Master Mix II (Applied Biosystems) was used to perform the reaction together with primers (for studying the expression of p53-regulated downstream genes) purchased from Invitrogen (Life Technologies). Relative mRNA quantification was obtained using the comparative Ct method ($\Delta\Delta$Ct), where GAPDH and β-actin genes served as internal controls.

In vitro transcription

In vitro transcription reactions were carried out essentially as described previously (42, 57) using 50 ng of G-less DNA templates. H1299 nuclear extracts along with purified p53 from the desired cell lines (by two rounds of immunoprecipitation) and template DNA were preincubated at room temperature for 10 min before nucleotides were added to the mixture. Reaction mixtures (20 μl) contained 2.5 mM NaF, 0.5 mM orthovanadate,

10 mM HEPES (pH 7.9), 12 mM Tris (pH 8.0), 0.1 mM EDTA, 12% glycerol, 60 mM KCl, 5 mM MgCl$_2$, 0.5 mM ATP, 0.5 mM UTP, 20 μM CTP, 0.25 mM *O*-methyl-GTP, 5 mM creatine phosphate, and 10 μM HO-3867. The DNA template contains six p53 DNA binding sites at the *p21/WAF* gene promoter upstream of the AdML (adenovirus major late) core promoter (57), a transcription initiation signal attached to a G-less cassette (which gives rise to transcripts of 440 nucleotides), a poly(A) signal, and finally a stop signal (CCT). Quantitative detection of the transcripts was done by converting the transcript to a cDNA form using poly(T) primers followed by qPCR using extension primers.

Immunoblotting

Tissue (tumor grafts) and cells (both untreated and treated) were harvested, and the protein was isolated using a total protein extraction kit from Millipore. They were then incubated on ice for 60 min followed by microcentrifugation at 10,000 $\times$ *g* for 15 min at 4°C. Aliquots of 40 μg of protein from each sample were boiled in sample preparation buffer from Invitrogen. The protein samples were separated on 10% polyacrylamide gels (Bio-Rad) and transferred to nitrocellulose membranes using the iBlot system (Invitrogen). After blocking in 5% milk in TBST (Tris-buffered saline with Tween 20), the membrane was probed with primary antibody (for the desired protein) overnight at 4 °C. The membranes were washed three times with TBST for 10 min, incubated with the appropriate secondary antibodies, and probed with primary antibodies for the desired protein. The membranes were incubated overnight at 4°C with the primary antibodies followed by incubation with secondary antibodies for 1 h and detected by a diaminobenzidine substrate kit (DAB, Thermo Scientific).

Detection of p53 mutations in liver, breast, and colon cancer tissues

The cDNA was prepared from total RNA isolated from breast, colon, and liver cancer tissues as shown in Fig. 1*b*. This cDNA was used as a template to amplify the DNA-binding domain of p53 as follows: Forward primer: 5′-CCTTCCCAGAAAACCTACCA-GGGCAGC-3′; and Reverse primer: 5′-TTTCTTGCGGAGA-TTCTCTTCCTCTG-3′ (with an expected amplicon length of 585 bp). The PCR products were gel-purified and subjected to automated DNA sequencing with ultra-HPLC purification (Stab Vida, Lisbon, Portugal). The mutations detected in the p53 DNA-binding domain from different tissues are shown in Fig. 1*c*.

Immunoprecipitation

Cells, both untreated and treated (for 24 h), were washed with PBS, harvested, and lysed in radioimmune precipitation buffer (50 mM Tris-HCl, pH 7.4, 150 mM NaCl, 1.0% (v/v) Triton X-100, 0.1% SDS, and 1.0% sodium deoxycholate) by incubating them on ice for 30 min followed by centrifugation at 9200 $\times$ *g* for 20 min. The whole-cell lysate (1 mg) was precleared with protein G PLUS-agarose beads and incubated with 5 μg of anti-mouse p53 WT conformation 1620 and p53 MT conformation 240 monoclonal antibodies on ice for 2 h. Then 10 μl of protein G PLUS-agarose was added to the lysate followed by further incubation at 4 °C for 4 h. After washing three

times with Nonidet P-40 buffer (20 mM Tris-HCl, pH 7.4, 100 mM NaCl, 10% (v/v) glycerol, 1.0% (v/v) Nonidet P-40, and 1 mM EDTA) and once with radioimmune precipitation buffer, the beads were resuspended in the sample buffer, boiled for 5 min, and loaded on to SDS-PAGE (10% gel). Transfer of proteins to nitrocellulose membranes was performed using the iBlot system (Invitrogen), and the membranes were then stripped and immunoblotted using anti-p53 (FL-393) polyclonal antibody.

References

1. Bieging, K. T., Mello, S. S., and Attardi, L. D. (2014) Unravelling mechanisms of p53-mediated tumour suppression. *Nat. Rev. Cancer* **14,** 359–370 CrossRef Medline
2. Weissmueller, S., Manchado, E., Saborowski, M., Morris J. P., 4th, Wagenblast, E., Davis, C. A., Moon, S. H., Pfister, N. T., Tschaharganeh, D. F., Kitzing, T., Aust, D., Markert, E. K., Wu, J., Grimmond, S. M., Pilarsky, C., *et al.* (2014) Mutant p53 drives pancreatic cancer metastasis through cell-autonomous PDGF receptor β signaling. *Cell* **157,** 382–394 CrossRef Medline
3. Muller, P. A., and Vousden, K. H. (2014) Mutant p53 in cancer: New functions and therapeutic opportunities. *Cancer Cell* **25,** 304–317 CrossRef Medline
4. Toledo, F., Krummel, K. A., Lee, C. J., Liu, C. W., Rodewald, L. W., Tang, M., and Wahl, G. M. (2006) A mouse p53 mutant lacking the proline-rich domain rescues Mdm4 deficiency and provides insight into the Mdm2-Mdm4-p53 regulatory network. *Cancer Cell* **9,** 273–285 CrossRef Medline
5. Vousden, K. H., and Ryan, K. M. (2009) p53 and metabolism. *Nat. Rev. Cancer* **9,** 691–700 CrossRef Medline
6. Bensaad, K., Tsuruta, A., Selak, M. A., Vidal, M. N., Nakano, K., Bartrons, R., Gottlieb, E., and Vousden, K. H. (2006) TIGAR, a p53-inducible regulator of glycolysis and apoptosis. *Cell* **126,** 107–120 CrossRef Medline
7. Madan, E., Gogna, R., Kuppusamy, P., Bhatt, M., Pati, U., and Mahdi, A. A. (2012) TIGAR induces p53-mediated cell-cycle arrest by regulation of RB-E2F1 complex. *Br. J. Cancer* **107,** 516–526 CrossRef Medline
8. Madan, E., Gogna, R., Bhatt, M., Pati, U., Kuppusamy, P., and Mahdi, A. A. (2011) Regulation of glucose metabolism by p53: Emerging new roles for the tumor suppressor. *Oncotarget* **2,** 948–957 Medline

9. Madan, E., Gogna, R., Kuppusamy, P., Bhatt, M., Mahdi, A. A., and Pati, U. (2013) SCO2 induces p53-mediated apoptosis by Thr845 phosphorylation of ASK-1 and dissociation of the ASK-1-Trx complex. *Mol. Cell. Biol.* **33,** 1285–1302 CrossRef Medline

10. Matoba, S., Kang, J. G., Patino, W. D., Wragg, A., Boehm, M., Gavrilova, O., Hurley, P. J., Bunz, F., and Hwang, P. M. (2006) p53 regulates mitochondrial respiration. *Science* **312,** 1650–1653 CrossRef Medline

11. Hadjal, Y., Hadadeh, O., Yazidi, C. E., Barruet, E., and Binétruy, B. (2013) A p38MAPK-p53 cascade regulates mesodermal differentiation and neurogenesis of embryonic stem cells. *Cell Death Dis.* **4,** e737 CrossRef Medline

12. Lujambio, A., Akkari, L., Simon, J., Grace, D., Tschaharganeh, D. F., Bolden, J. E., Zhao, Z., Thapar, V., Joyce, J. A., Krizhanovsky, V., and Lowe, S. W. (2013) Non-cell-autonomous tumor suppression by p53. *Cell* **153,** 449–460 CrossRef Medline

13. Bourdon, J. C., Fernandes, K., Murray-Zmijewski, F., Liu, G., Diot, A., Xirodimas, D. P., Saville, M. K., and Lane, D. P. (2005) p53 isoforms can regulate p53 transcriptional activity. *Genes Dev.* **19,** 2122–2137 CrossRef Medline

14. Jordan, J. J., Inga, A., Conway, K., Edmiston, S., Carey, L. A., Wu, L., and Resnick, M. A. (2010) Altered-function p53 missense mutations identified in breast cancers can have subtle effects on transactivation. *Mol. Cancer Res.* **8,** 701–716 CrossRef Medline

15. Trbusek, M., Smardova, J., Malcikova, J., Sebejova, L., Dobes, P., Svitakova, M., Vranova, V., Mraz, M., Francova, H. S., Doubek, M., Brychtova, Y., Kuglik, P., Pospisilova, S., and Mayer, J. (2011) Missense mutations located in structural p53 DNA-binding motifs are associated with extremely poor survival in chronic lymphocytic leukemia. *J. Clin. Oncol.* **29,** 2703–2708 CrossRef Medline

16. Kamada, R., Nomura, T., Anderson, C. W., and Sakaguchi, K. (2011) Cancer-associated p53 tetramerization domain mutants: Quantitative analysis reveals a low threshold for tumor suppressor inactivation. *J. Biol. Chem.* **286,** 252–258 CrossRef Medline

17. Timofeev, O., Schlereth, K., Wanzel, M., Braun, A., Nieswandt, B., Pagenstecher, A., Rosenwald, A., Elsässer, H. P., and Stiewe, T. (2013) p53 DNA binding cooperativity is essential for apoptosis and tumor suppression *in vivo. Cell Rep.* **3,** 1512–1525 CrossRef Medline

18. Brázdová, M., Navrátilová, L., Tichý, V., Němcová, K., Lexa, M., Hrstka, R., Pečinka, P., Adámik, M., Vojtesek, B., Paleček, E., Deppert, W., and Fojta, M. (2013) Preferential binding of hot spot mutant p53 proteins to supercoiled DNA *in vitro* and in cells. *PLoS ONE* **8,** e59567 CrossRef Medline

19. Chan, W. M., Siu, W. Y., Lau, A., and Poon, R. Y. (2004) How many mutant p53 molecules are needed to inactivate a tetramer? *Mol. Cell. Biol.* **24,** 3536–3551 CrossRef Medline

20. Coates, A. S., Millar, E. K., O'Toole, S. A., Molloy, T. J., Viale, G., Goldhirsch, A., Regan, M. M., Gelber, R. D., Sun, Z., Castiglione-Gertsch, M., Gusterson, B., Musgrove, E. A., and Sutherland, R. L. (2012) Prognostic interaction between expression of p53 and estrogen receptor in patients with node-negative breast cancer: Results from IBCSG Trials VIII and IX. *Breast Cancer Res.* **14,** R143 CrossRef Medline

21. Yang, P., Du, C. W., Kwan, M., Liang, S. X., and Zhang, G. J. (2013) The impact of p53 in predicting clinical outcome of breast cancer patients with visceral metastasis. *Sci. Rep.* **3,** 2246 CrossRef Medline

22. Morton, J. P., Timpson, P., Karim, S. A., Ridgway, R. A., Athineos, D., Doyle, B., Jamieson, N. B., Oien, K. A., Lowy, A. M., Brunton, V. G., Frame, M. C., Evans, T. R., and Sansom, O. J. (2010) Mutant p53 drives metastasis and overcomes growth arrest/senescence in pancreatic cancer. *Proc. Natl. Acad. Sci. U.S.A.* **107,** 246–251 CrossRef Medline

23. Peraud, A., Kreth, F. W., Wiestler, O. D., Kleihues, P., and Reulen, H. J. (2002) Prognostic impact of TP53 mutations and P53 protein overexpression in supratentorial WHO grade II astrocytomas and oligoastrocytomas. *Clin. Cancer Res.* **8,** 1117–1124 Medline

24. Ahrendt, S. A., Hu, Y., Buta, M., McDermott, M. P., Benoit, N., Yang, S. C., Wu, L., and Sidransky, D. (2003) p53 mutations and survival in stage I non-small-cell lung cancer: results of a prospective study. *J. Natl. Cancer Inst.* **95,** 961–970 CrossRef Medline

25. Muller, P. A., and Vousden, K. H. (2013) p53 mutations in cancer. *Nat. Cell Biol.* **15,** 2–8 CrossRef Medline

26. Lim, L. Y., Vidnovic, N., Ellisen, L. W., and Leong, C. O. (2009) Mutant p53 mediates survival of breast cancer cells. *Br J Cancer* **101,** 1606–1612 CrossRef Medline

27. Kirn, D. (2001) Clinical research results with dl1520 (Onyx-015), a replication-selective adenovirus for the treatment of cancer: What have we learned? *Gene Ther.* **8,** 89–98 CrossRef Medline

28. Makower, D., Rozenblit, A., Kaufman, H., Edelman, M., Lane, M. E., Zwiebel, J., Haynes, H., and Wadler, S. (2003) Phase II clinical trial of intralesional administration of the oncolytic adenovirus ONYX-015 in patients with hepatobiliary tumors with correlative p53 studies. *Clin. Cancer Res.* **9,** 693–702 Medline

29. Swisher, S. G., Roth, J. A., Nemunaitis, J., Lawrence, D. D., Kemp, B. L., Carrasco, C. H., Connors, D. G., El-Naggar, A. K., Fossella, F., Glisson, B. S., Hong, W. K., Khuri, F. R., Kurie, J. M., Lee, J. J., Lee, J. S., *et al.* (1999) Adenovirus-mediated p53 gene transfer in advanced non-small-cell lung cancer. *J. Natl. Cancer Inst.* **91,** 763–771 CrossRef Medline

30. Khoo, K. H., Verma, C. S., and Lane, D. P. (2014) Drugging the p53 pathway: Understanding the route to clinical efficacy. *Nat. Rev. Drug Discov.* **13,** 217–236 CrossRef Medline

31. Gogna, R., Madan, E., Kuppusamy, P., and Pati, U. (2012) Re-oxygenation causes hypoxic tumor regression through restoration of p53 wild-type conformation and post-translational modifications. *Cell Death Dis.* **3,** e286 CrossRef Medline

32. Gogna, R., Madan, E., Kuppusamy, P., and Pati, U. (2012) Chaperoning of mutant p53 protein by wild-type p53 protein causes hypoxic tumor regression. *J. Biol. Chem.* **287,** 2907–2914 CrossRef Medline

33. Walerych, D., Olszewski, M. B., Gutkowska, M., Helwak, A., Zylicz, M., and Zylicz, A. (2009) Hsp70 molecular chaperones are required to support p53 tumor suppressor activity under stress conditions. *Oncogene* **28,** 4284–4294 CrossRef Medline

34. Brown, C. J., Lain, S., Verma, C. S., Fersht, A. R., and Lane, D. P. (2009) Awakening guardian angels: Drugging the p53 pathway. *Nat. Rev. Cancer* **9,** 862–873 CrossRef Medline

35. Bullock, A. N., and Fersht, A. R. (2001) Rescuing the function of mutant p53. *Nat. Rev. Cancer* **1,** 68–76 CrossRef Medline

36. Yu, X., Vazquez, A., Levine, A. J., and Carpizo, D. R. (2012) Allele-specific p53 mutant reactivation. *Cancer Cell* **21,** 614–625 CrossRef Medline

37. Selivanova, G., and Wiman, K. G. (2007) Reactivation of mutant p53: Molecular mechanisms and therapeutic potential. *Oncogene* **26,** 2243–2254 CrossRef Medline

38. Lehmann, B. D., and Pietenpol, J. A. (2012) Targeting mutant p53 in human tumors. *J. Clin. Oncol.* **30,** 3648–3650 CrossRef Medline

39. Lehmann, S., Bykov, V. J., Ali, D., Andrén, O., Cherif, H., Tidefelt, U., Uggla, B., Yachnin, J., Juliusson, G., Moshfegh, A., Paul, C., Wiman, K. G., and Andersson, P. O. (2012) Targeting p53 *in vivo*: A first-in-human study with p53-targeting compound APR-246 in refractory hematologic malignancies and prostate cancer. *J. Clin. Oncol.* **30,** 3633–3639 CrossRef Medline

40. Lambert, J. M., Gorzov, P., Veprintsev, D. B., Söderqvist, M., Segerbäck, D., Bergman, J., Fersht, A. R., Hainaut, P., Wiman, K. G., and Bykov, V. J. (2009) PRIMA-1 reactivates mutant p53 by covalent binding to the core domain. *Cancer Cell* **15,** 376–388 CrossRef Medline

41. Liang, Y., Besch-Williford, C., and Hyder, S. M. (2009) PRIMA-1 inhibits growth of breast cancer cells by re-activating mutant p53 protein. *Int. J. Oncol.* **35,** 1015–1023 Medline

42. Shieh, S. Y., Ikeda, M., Taya, Y., and Prives, C. (1997) DNA damage-induced phosphorylation of p53 alleviates inhibition by MDM2. *Cell* **91,** 325–334 CrossRef Medline

43. Issaeva, N., Bozko, P., Enge, M., Protopopova, M., Verhoef, L. G., Masucci, M., Pramanik, A., and Selivanova, G. (2004) Small molecule RITA binds to p53, blocks p53-HDM-2 interaction and activates p53 function in tumors. *Nat. Med.* **10,** 1321–1328 CrossRef Medline

44. Krajewski, M., Ozdowy, P., D'Silva, L., Rothweiler, U., and Holak, T. A. (2005) NMR indicates that the small molecule RITA does not block p53-MDM2 binding *in vitro. Nat. Med.* **11,** 1135–1136

45. Hiraki, M., Hwang, S. Y., Cao, S., Ramadhar, T. R., Byun, S., Yoon, K. W., Lee, J. H., Chu, K., Gurkar, A. U., Kolev, V., Zhang, J., Namba, T., Murphy, M. E., Newman, D. J., Mandinova, A., *et al.* (2015) Small-molecule reacti-

vation of mutant p53 to wild-type-like p53 through the p53-Hsp40 regulatory axis. *Chem. Biol.* **22,** 1206–1216 CrossRef Medline

46. Staab, A., Loeffler, J., Said, H. M., Diehlmann, D., Katzer, A., Beyer, M., Fleischer, M., Schwab, F., Baier, K., Einsele, H., Flentje, M., and Vordermark, D. (2007) Effects of HIF-1 inhibition by chetomin on hypoxia-related transcription and radiosensitivity in HT 1080 human fibrosarcoma cells. *BMC Cancer* **7,** 213 CrossRef Medline

47. Foster, B. A., Coffey, H. A., Morin, M. J., and Rastinejad, F. (1999) Pharmacological rescue of mutant p53 conformation and function. *Science* **286,** 2507–2510 CrossRef Medline

48. Rippin, T. M., Bykov, V. J., Freund, S. M., Selivanova, G., Wiman, K. G., and Fersht, A. R. (2002) Characterization of the p53-rescue drug CP-31398 in vitro and in living cells. *Oncogene* **21,** 2119–2129 CrossRef Medline

49. Wischhusen, J., Naumann, U., Ohgaki, H., Rastinejad, F., and Weller, M. (2003) CP-31398, a novel p53-stabilizing agent, induces p53-dependent and p53-independent glioma cell death. *Oncogene* **22,** 8233–8245 CrossRef Medline

50. Selvendiran, K., Ahmed, S., Dayton, A., Ravi, Y., Kuppusamy, M. L., Bratasz, A., Rivera, B. K., Kálai, T., Hideg, K., and Kuppusamy, P. (2010) HO-3867, a synthetic compound, inhibits the migration and invasion of ovarian carcinoma cells through downregulation of fatty acid synthase and focal adhesion kinase. *Mol. Cancer Res.* **8,** 1188–1197 CrossRef Medline

51. Hu, Y., Zhao, C., Zheng, H., Lu, K., Shi, D., Liu, Z., Dai, X., Zhang, Y., Zhang, X., Hu, W., and Liang, G. (2017) A novel STAT3 inhibitor HO-3867 induces cell apoptosis by reactive oxygen species-dependent endoplasmic reticulum stress in human pancreatic cancer cells. *Anticancer Drugs* **28,** 392–400 CrossRef Medline

52. Rath, K. S., Naidu, S. K., Lata, P., Bid, H. K., Rivera, B. K., McCann, G. A., Tierney, B. J., Elnaggar, A. C., Bravo, V., Leone, G., Houghton, P., Hideg, K., Kuppusamy, P., Cohn, D. E., and Selvendiran, K. (2014) HO-3867, a safe STAT3 inhibitor, is selectively cytotoxic to ovarian cancer. *Cancer Res.* **74,** 2316–2327 CrossRef Medline

53. Selvendiran, K., Tong, L., Bratasz, A., Kuppusamy, M. L., Ahmed, S., Ravi, Y., Trigg, N. J., Rivera, B. K., Kálai, T., Hideg, K., and Kuppusamy, P. (2010) Anticancer efficacy of a difluorodiarylidenyl piperidone (HO-3867) in human ovarian cancer cells and tumor xenografts. *Mol. Cancer Ther.* **9,** 1169–1179 CrossRef Medline

54. Tierney, B. J., McCann, G. A., Cohn, D. E., Eisenhauer, E., Sudhakar, M., Kuppusamy, P., Hideg, K., and Selvendiran, K. (2012) HO-3867, a STAT3 inhibitor induces apoptosis by inactivation of STAT3 activity in BRCA1-mutated ovarian cancer cells. *Cancer Biol. Ther.* **13,** 766–775 CrossRef Medline

55. Jackson, J. G., and Pereira-Smith, O. M. (2006) p53 is preferentially recruited to the promoters of growth arrest genes p21 and GADD45 during replicative senescence of normal human fibroblasts. *Cancer Res.* **66,** 8356–8360 CrossRef Medline

56. Vojtesek, B., Dolezalova, H., Lauerova, L., Svitakova, M., Havlis, P., Kovarik, J., Midgley, C. A., and Lane, D. P. (1995) Conformational changes in p53 analysed using new antibodies to the core DNA binding domain of the protein. *Oncogene* **10,** 389–393 Medline

57. Thomas, M. C., and Chiang, C. M. (2005) E6 oncoprotein represses p53-dependent gene activation via inhibition of protein acetylation independently of inducing p53 degradation. *Mol. Cell* **17,** 251–264 CrossRef Medline

58. Turin, I., Schiavo, R., Maestri, M., Luinetti, O., Bello, B., Paulli, M., Dionigi, P., Roccio, M., Spinillo, A., Ferulli, F., Tanzi, M., Maccario, R., Montagna, D., and Pedrazzoli, P. (2014) *In vitro* efficient expansion of tumor cells deriving from different types of human tumor samples. *Med. Sci.* **2,** 70–81 CrossRef

59. Wilcken, R., Liu, X., Zimmermann, M. O., Rutherford, T. J., Fersht, A. R., Joerger, A. C., and Boeckler, F. M. (2012) Halogen-enriched fragment libraries as leads for drug rescue of mutant p53. *J. Am. Chem. Soc.* **134,** 6810–6818 CrossRef Medline

60. Bauer, M. R., Joerger, A. C., and Fersht, A. R. (2016) 2-Sulfonylpyrimidines: Mild alkylating agents with anticancer activity toward p53-compromised cells. *Proc. Natl. Acad. Sci. U.S.A.* **113,** E5271–E5280 CrossRef Medline

61. Gogna, R., Madan, E., Khan, M., Pati, U., and Kuppusamy, P. (2013) p53's choice of myocardial death or survival: Oxygen protects infarct myocardium by recruiting p53 on NOS3 promoter through regulation of p53-Lys(118) acetylation. *EMBO Mol. Med.* **5,** 1662–1683 CrossRef Medline

62. Madan, E., Gogna, R., and Pati, U. (2012) p53 Ser15 phosphorylation disrupts the p53–RPA70 complex and induces RPA70-mediated DNA repair in hypoxia. *Biochem. J.* **443,** 811–820 CrossRef Medline